JVSTA Journal of Vacuum Science & Technology A

Properties of nanostructured undoped ZrO2 thin film electrolytes by plasma enhanced atomic layer deposition for thin film solid oxide fuel cells

Gu Young Cho, Seungtak Noh, Yoon Ho Lee, Sanghoon Ji, Soon Wook Hong, Bongjun Koo, Jihwan An, Young-Beom Kim, and Suk Won Cha

Citation: Journal of Vacuum Science & Technology A **34**, 01A151 (2016); doi: 10.1116/1.4938105
View online: http://dx.doi.org/10.1116/1.4938105
View Table of Contents: http://scitation.aip.org/content/avs/journal/jvsta/34/1?ver=pdfcov
Published by the AVS: Science & Technology of Materials, Interfaces, and Processing

Properties of nanostructured undoped ZrO_2 thin film electrolytes by plasma enhanced atomic layer deposition for thin film solid oxide fuel cells

Gu Young Cho, Seungtak Noh, and Yoon Ho Lee
Department of Mechanical and Aerospace Engineering, Seoul National University, 1 Gwanak-ro, Gwanak-gu, Seoul 151-744, Republic of Korea

Sanghoon Ji
Graduate School of Convergence Science and Technology, Seoul National University, Iui-dong, Yeongtong-gu, Suwon 443-270, Republic of Korea

Soon Wook Hong and Bongjun Koo
Department of Mechanical Engineering, Hanyang University, 222 Wangsimni-ro, Seongdong-gu, Seoul 133-791, Republic of Korea

Jihwan An
Manufacturing Systems and Design Engineering Programme, Seoul National University of Science and Technology, 232 Gongneung-ro, Nowon-gu, Seoul 139-743, Republic of Korea

Young-Beom Kim[a)]
Department of Mechanical Engineering, Hanyang University, 222 Wangsimni-ro, Seongdong-gu, Seoul 133-791, Republic of Korea

Suk Won Cha[a)]
Department of Mechanical and Aerospace Engineering, Seoul National University, 1 Gwanak-ro, Gwanak-gu, Seoul 151-744, Republic of Korea

(Received 30 August 2015; accepted 7 December 2015; published 28 December 2015)

Nanostructured ZrO_2 thin films were prepared by thermal atomic layer deposition (ALD) and by plasma-enhanced atomic layer deposition (PEALD). The effects of the deposition conditions of temperature, reactant, plasma power, and duration upon the physical and chemical properties of ZrO_2 films were investigated. The ZrO_2 films by PEALD were polycrystalline and had low contamination, rough surfaces, and relatively large grains. Increasing the plasma power and duration led to a clear polycrystalline structure with relatively large grains due to the additional energy imparted by the plasma. After characterization, the films were incorporated as electrolytes in thin film solid oxide fuel cells, and the performance was measured at 500 °C. Despite similar structure and cathode morphology of the cells studied, the thin film solid oxide fuel cell with the ZrO_2 thin film electrolyte by the thermal ALD at 250 °C exhibited the highest power density (38 mW/cm^2) because of the lowest average grain size at cathode/electrolyte interface. © *2015 American Vacuum Society*. [http://dx.doi.org/10.1116/1.4938105]

I. INTRODUCTION

Zirconium oxide (Zirconia, ZrO_2) or ZrO_2 based materials are well-known materials used as dielectric layers in semiconductor devices or as a fundamental material for oxygen ion-conducting electrolytes in solid oxide fuel cells (SOFCs), such as yttria-stabilized zirconia (YSZ) or scandia-stabilized zirconia. ZrO_2-based materials are widely used as SOFC electrolytes due to their superior chemical stability and mechanical strength compared with other electrolyte materials such as doped CeO_2.[1–8] Thin film SOFCs (TF-SOFCs) can be operated at lower temperature (350–500 °C) than conventional SOFCs; the use of thin film electrodes and electrolyte in these devices counterbalances the significant drop in performance arising from the use of a lower operating temperature. Because the TF-SOFC uses electrolyte of nanometer-scale thickness, the formation of pinhole-type microstructural defects during fabrication or other gas leak issues have emerged as crucial problems.[4,9,10] The requirement of pinhole-free thin film electrolyte is especially critical for TF-SOFCs that use anode-supporting structures such as anodic aluminum oxide (AAO), due to its inherently rough surface, including regularly distributed nanoholes.[4,9,11–18]

To fabricate the necessary pinhole-free, gas-tight and dense thin film electrolytes or functional layers, atomic layer deposition (ALD) and plasma enhanced atomic layer deposition (PEALD) have been widely used to fabricate ZrO_2 or YSZ thin films in previous researches due to these techniques' inherent advantages of high uniformity, superior step coverage, and improved density of films relative to other thin film deposition techniques.[1–3,6,9,11–13,16,19–22] Moreover, the use of ALD or PEALD to deposit ZrO_2 thin films allows flexibility in the choice of deposition temperature, due to the relatively low boiling temperature of the Zr precursor and the wide ALD window.[23–25] Therefore, it is easy to study the effects of deposition temperature upon the resulting properties of the nanostructured ZrO_2 electrolyte prepared by ALD

[a)]Authors to whom correspondence should be addressed; electronic addresses: ybkim@hanyang.ac.kr; swcha@snu.ac.kr

or PEALD. In addition, when ALD or PEALD is used, it is easy to apply various ZrO_2 thin films with specific characteristics due to the simplicity of control available over other deposition conditions such as the types of oxidant used, the plasma power, and the plasma time.

The aforementioned previous studies investigated only thermal ALD ZrO_2 or YSZ thin films as thin film electrolytes or functional layers.[1,2,6,9,11–13,16,19–22] However, most of prior researches used YSZ films prepared by thermal ALD as thin film electrolytes and cathode functional layers because of better ionic conductivity and higher oxygen vacancies,[1,2,6,9,11–13,16,19,20] or utilized pure ZrO_2 films as functional layers to improve performance and long-term durability of fuel cells.[21,22] There have been no researches about the physical, chemical, and electrochemical properties of PEALD ZrO_2 as a thin film electrolyte of TF-SOFCs.

In this study, to investigate the effects of deposition conditions upon the resulting properties of ZrO_2 films, nanostructured ZrO_2 thin films were prepared by both thermal ALD and PEALD, using various deposition conditions. The physical and chemical properties of the nanostructured ZrO_2 thin films were characterized. Then, the films were incorporated into AAO-based TF-SOFCs as the thin film electrolytes, and their electrochemical characteristics were evaluated in this application. The impurity content and crystallinity of ZrO_2 thin films were improved when PEALD was used, due to the superior reactivity of the plasma species in this technique. The average surface grain size increased as the plasma power or time increased. Interestingly, TF-SOFCs incorporating ZrO_2 thin film electrolytes formed by using the conventional thermal ALD performed best among the samples studied, possibly due to the effects of their small surface grains upon the cathode kinetics.

II. EXPERIMENT

A. Preparation and characterization of ZrO_2 thin films

A commercial showerhead-type direct plasma-enhanced atomic layer deposition system equipped with a capacitively coupled plasma power source (Atomic premium, CN-1 Co., Korea) was utilized to synthesize ZrO_2 thin films. A commercial tetrakis(dimethylamino)zirconium precursor (TDMAZ, Sigma Aldrich, USA) was used as the Zr source. High-purity Ar gas (99.999%, Shinjin Gas, Korea) was used as carrier gas and purge gas. Pure O_2 gas (99.999%, Shinjin Gas, Korea) was used as a reactant and as the O_2 plasma source gas. The temperature of the stainless steel canister and gas delivery line were, respectively, maintained at 50 and 70 °C during deposition. Synthesis of ZrO_2 thin films was conducted at 100 and 250 °C to study the effects of deposition temperature upon the properties of the resulting ZrO_2 films. Each PEALD ZrO_2 deposition cycle comprised the following steps: (1) Zr precursor pulse (3 s), (2) Ar purging (30 s), (3) O_2 pulse (1 s), (4) O_2 pulse with plasma (2 or 8 s), and (5) Ar purging (30 s). Step (3) was added to allow stabilization of the O_2 partial pressure in the chamber prior to step (4). Various conditions of applied plasma power and plasma time were used to investigate the influence of these conditions upon the properties of the resulting ZrO_2 films. When thermal ALD was used, in which O_2 gas was the only reactant used, steps (3) and (4) were combined as an 8 s O_2 pulse step with no plasma.

To study the differences in the properties of ZrO_2 thin films formed using the different deposition methods (PEALD and thermal ALD), ZrO_2 films were deposited on Si wafer substrates (LG Siltron Co., Korea) under various conditions, and the characteristics of the resulting films were analyzed. Before deposition, the Si wafers were sequentially cleaned with acetone, ethanol, and deionized water for 10 min each to remove surface contamination. The chemical compositions of the ZrO_2 films were characterized by using x-ray photoelectron spectroscopy (XPS, Theta Probe base system, Thermo Fisher Scientific, USA, 1486.6 eV Al Kα source, 400 μm spot diameter). The surface of ZrO_2 thin films were cleaned by using 150 eV Ar ion etching for 30 s before measurements to remove surface impurities. The crystallinity of the ZrO_2 thin films was measured by a glancing-mode x-ray diffraction (XRD, X'pert Pro, PANalytical, Netherlands, Cu Kα source). The crystal structure of the ZrO_2 thin films was studied by comparison to ICDD-JCPDS Card Nos. 01-080-0965, 00-027-0997, and 00-036-0420. The grain size, surface topography, and root mean square (RMS) roughness were studied by using noncontact-mode atomic force microscopy (AFM, XE 150, Park Systems, Korea). Image processing of the AFM micrographs and calculation of the ZrO_2 thin films' grain sizes were conducted by using a commercial software (XEI, Park Systems, Korea).

B. Fabrication and characterization of TF-SOFCs

Commercial AAO (Synkera Co., USA) templates of 100 μm thickness were used as substrates for the fabrication of TF-SOFCs. Detailed information on these templates has been reported previously.[9,12,13] A dense Pt anode was deposited onto each AAO template by using a commercial sputtering system (A-tech Co., Korea) to form a smooth surface prior to deposition of the electrolyte. The 300 nm thick dense Pt anodes were prepared by a direct current (DC) sputtering technique conducted using the sputtering power of 200 W under 0.67 Pa of pure Ar. The nanostructured ZrO_2 thin film electrolytes were then synthesized on the dense Pt anodes by means of PEALD or thermal ALD ($\sim$100 nm). Finally, 150 nm thick porous Pt cathodes were deposited onto the electrolyte layers by using DC sputtering, conducted using the sputtering power of 100 W under 12 Pa of pure Ar to maximize the triple phase boundary length.

The electrochemical characterizations of TF-SOFCs were conducted at 500 °C by using a custom measurement setup developed in our laboratory.[9,12,13] Pure H_2 of 100 sccm was supplied to the Pt anode as the fuel, and stationary air was used as the oxidant. A combined potentiostat/galvanostat and frequency response analyzer instrument (Solartron 1287/1260, Solartron Co., UK) was used to evaluate electrochemical characteristics of the TF-SOFCs such as open circuit voltage (OCV) and current–voltage behavior, and to carry out electrochemical impedance spectroscopy (EIS).

EIS of TF-SOFCs was conducted under OCV and 0.5 V DC bias conditions with 50 mV of amplitude voltage over the frequency range from 2 MHz to 2 Hz. The results of EIS measurements were analyzed by using the ZPlot software. The cross-sectional structures of TF-SOFCs and their cathode surfaces were analyzed by focused ion beam scanning electron spectroscopy (FIB-SEM, Quanta 3D, FEI, USA) using the operating voltage of 5 kV.

III. RESULTS AND DISCUSSION

A. Characteristics of ZrO_2 thin films

Various characterizations of the nanostructured ZrO_2 thin films were carried out prior to their application as electrolytes of TF-SOFCs. Table I summarizes the various deposition conditions used for preparing the ZrO_2 thin films by means of PEALD and thermal ALD; the deposition conditions of the reactant used (O_2 plasma versus O_2 gas), the deposition temperature (100 vs 250 °C), the plasma power (50 vs 200 W), and the plasma duration (2 vs 8 s) were changed to evaluate the influences of these conditions upon the physical and chemical characteristics of the resulting ZrO_2 thin films.

Table II lists the results of XPS measurements of the ZrO_2 thin films deposited under the various conditions used. The chemical compositions of the ZrO_2 thin films deposited by PEALD were very similar regardless of the deposition conditions used, and included very low carbon content (<1.5 at. %) and nitrogen content (<0.5 at. %). These low contaminant concentrations can be explained as a result of the effective removal of ligands by highly reactive oxygen plasma species.[23,26,27] That is, to say, ligands composed of C, H, and N in the TDMAZ precursor were removed nearly completely by the oxygen plasma during the PEALD process, resulting in the deposition of high-quality ZrO_2 thin films.

In comparison, when the thermal ALD was conducted at 250 °C (use O_2 as a reactant at 250 °C; hereafter termed T-250), the resulting ZrO_2 contained more than 3.5 times the carbon contaminants (5.49 at. %) and five times the nitrogen contaminants (2.58 at. %) because of the poor reactivity of O_2 gas in the ligand exchange process.

XRD analyses were conducted of the as-deposited ZrO_2 samples to determine their crystallinity and orientation; the results are given in Fig. 1. ZrO_2 thin films prepared by thermal ALD showed nanocrystalline structure (very small peaks), which is consistent with earlier reports.[2] However, ZrO_2 films by PEALD showed polycrystalline structure. In contrast to the sample by thermal ALD, the film prepared by PEALD at 50 W, 2 s, and 100 °C (hereafter termed P-50-100) showed clear and narrow XRD peaks corresponding to the tetragonal phase. This phenomenon occurred because the additional energy provided to the film by ion bombardment aided crystallization, even at low temperature for which little thermal energy is available.[26–28] The film prepared by PEALD at 50 W, 2 s, and 250 °C (hereafter termed P-50-250) yielded sharper and clearer peaks than P-50-100 due to the influence of thermal energy in aiding crystallization. Interestingly, in the case of the film prepared by PEALD at 200 W, 8 s, and 250 °C (hereafter termed P-200-250), many clear peaks corresponding to the monoclinic structure were observed.

Table I. Deposition conditions of ZrO_2 thin films.

	Temperature (°C)	Plasma power (W)	Plasma time (s)	
P-50-100	100	50	2	Low temperature
P-50-250	250	50	2	
P-200-250	250	200	8	High plasma power Long plasma time
T-250	250	—	—	Thermal O_2 reactant

Table II. Chemical compositions of ZrO_2 thin films.

	P-50-100	P-50-250	P-200-250	T-250
Temperature	100 °C		250 °C	
Reactant		O_2 plasma		O_2
Zr3d (at. %)	37.88	37.59	38.34	37.42
O1s (at. %)	61	60.84	59.84	54.5
C1s (at. %)	1.03	1.42	1.44	5.49
N1s (at. %)	0.09	0.14	0.38	2.58

Nanometric ZrO_2 with small crystallite size (<30 nm) has been previously reported to show tetragonal phase due to its lower surface free energy than the monoclinic phase in nanocrystallites.[4] Also, the tetragonal structure is transformed to monoclinic structure as the crystallite size is increased.[29,30]

Therefore, the monoclinic structure of the P-200-250 was caused by its larger grain size, which arose from the additional energy by the high-plasma power and long-duration.

The AFM images of the as-deposited ZrO_2 films prepared on Si wafers (Fig. 2) were acquired. The surface roughnesses of ZrO_2 thin films prepared by PEALD with 50 W of O_2 plasma were greater than those of ZrO_2 films deposited by thermal ALD, regardless of the temperature. Furthermore, the surface roughness of ZrO_2 films fabricated by PEALD increased as the deposition temperature was increased. This was probably due to the high crystallinity and growth rate of PEALD, arising from the superior reactivity of plasma species. Interestingly, the surface roughness of the P-200-250 was similar to that of T-250. We speculate that the low surface roughness arising when this high power and long duration was used probably occurred because of an etching effect caused by ion bombardment during the plasma process in the direct PEALD system.[26,27] It is generally known that direct PEALD systems deliver much higher energy to film surfaces than remote PEALD, due to the greater proximity between the substrates and the plasma generator.[26,27]

It is widely known that the surface grain size (i.e., density of grain boundary) of electrolyte has enormous influence on oxygen reduction reactions.[31–33] The average surface grain sizes of the as-deposited ZrO_2 thin films were measured based on the AFM images using the XEI software.

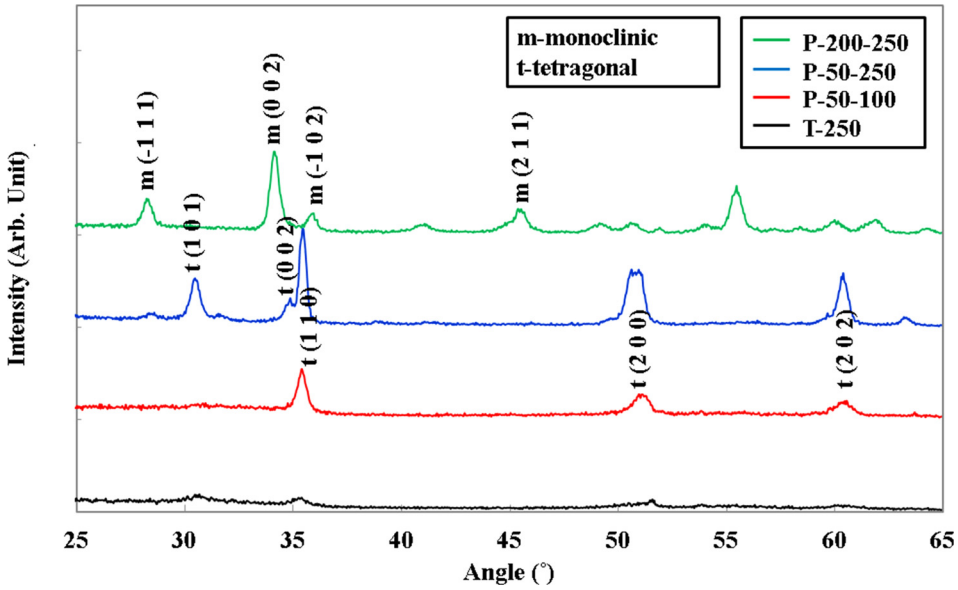

FIG. 1. (Color online) Crystal structures of the as-deposited ZrO_2 thin films.

The average surface grain size was 9.428 nm for T-250, 13.803 nm for P-50-100, 12.566 nm for P-50-250, and 15.416 nm for P-200-250. It is notable that the grain sizes of ZrO_2 films deposited by thermal ALD were much smaller than those of ZrO_2 films deposited by PEALD, regardless of the deposition temperature, plasma power, or plasma duration. Moreover, the average grain size of ZrO_2 thin films prepared by PEALD increased as the plasma power and time increased. Similar to the crystallinity trend, we believe that the additional energy supplied by bombardment of the film surface by plasma species aided the surface grain growth.[26–28]

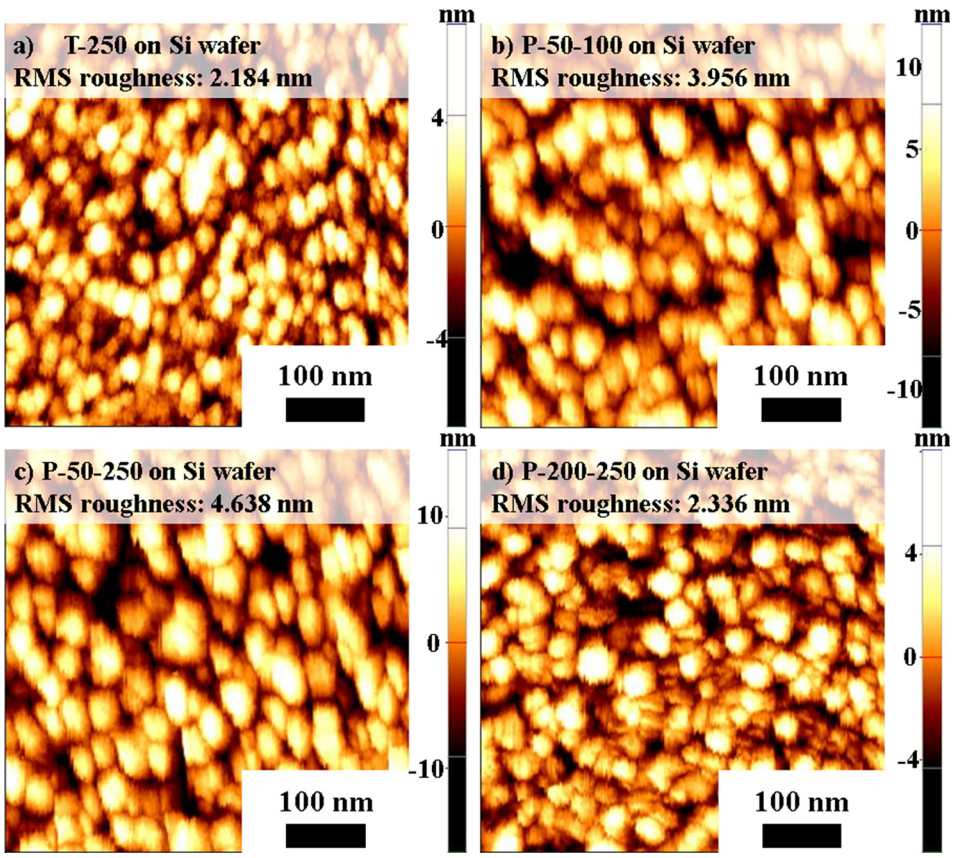

FIG. 2. (Color online) Surface topography of ZrO_2 thin films. (a) T-250; RMS roughness: 2.184 nm. (b) P-50-100; RMS roughness: 3.956 nm. (c) P-50-250; RMS roughness: 4.638 nm. (d) P-200-250; RMS roughness: 2.336 nm.

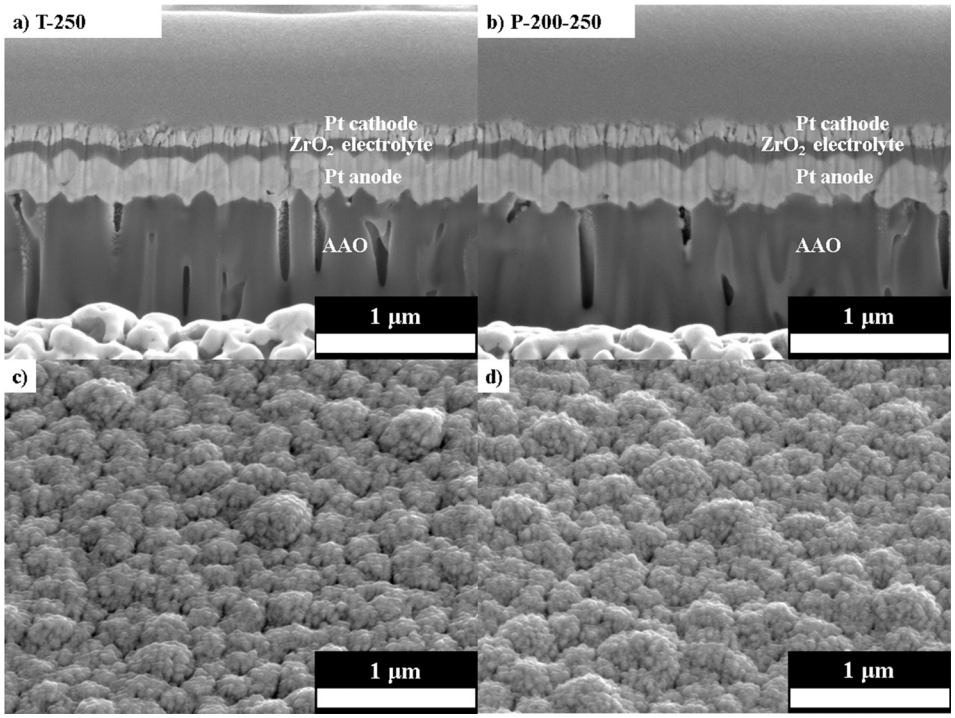

FIG. 3. FIB-SEM analysis results of TF-SOFCs. Cross-sectional images of TF-SOFCs based on (a) T-250 and (b) P-50-250. Surface morphology of cathodes of TF-SOFCs based on (c) T-250 and (d) P-50-250.

B. Characteristics of TF-SOFCs using undoped ZrO_2 thin film electrolyte

As mentioned above, all fuel cell samples were composed of the layered structure of dense Pt anode/nanostructured ZrO_2 thin film electrolyte/porous Pt cathode on the AAO template. To confirm the cross-sectional structure and surface morphology of TF-SOFCs, FIB-SEM analysis was conducted on fuel cells fabricated based on T-250 and on P-50-250 films. Figure 3 shows the cross-sectional structure and surface morphology of the porous Pt cathode of each fuel cell sample. In cross-sectional FIB-SEM images, very similar structures of the dense Pt anode, dense nanostructured ZrO_2 thin film electrolyte, and Pt cathode of each TF-SOFC were observed. In addition to their similar cell structures, the Pt cathodes of each fuel cell sample were observed to have a similar surface morphology. Despite the different deposition conditions used to form the nanostructured ZrO_2 thin film electrolytes, all TF-SOFCs studied here had similar cross-sectional structure and cathode surface morphology.

The polarization curves were acquired for the fuel cells based on the various electrolytes studied (Fig. 4). The peak power density of the fuel cell based on T-250 was much higher than that of the other TF-SOFCs based on electrolytes prepared by PEALD. The TF-SOFC based on the T-250 electrolyte demonstrated the highest performance at 500 °C, 38 mW/cm^2, which was 1.9 times that of the cell based on P-50-100 (20 mW/cm^2), 2.92 times that of the cell based on P-50-250 (13 mW/cm^2), and 3.8 times that of the cell based on P-200-250 (10 mW/cm^2).

These results were much lower compared with the results of free-standing TF-SOFCs with sputtered undoped ZrO_2 thin film electrolyte in previous study.[4] We observed that higher performance of the prior study caused differences in fabrication process (ALD and PEALD versus sputter), thinner electrolyte (~100 vs ~50 nm), and smaller active area (1×1 mm^2 vs 160×160 μm^2).

Interestingly, the polarization curves of the TF-SOFCs showed clear differences in the activation loss observed in the low current density region. These results probably arose from the cathodic activation loss that is caused by sluggish oxygen reduction reactions (ORRs) at a low operating temperature (500 °C).[1,4,12] Moreover, as mentioned above, it is generally known that surface grain size, that is, to say, the density of grain boundaries at the interface between the cathode and the electrolyte, greatly affects the oxygen kinetics.[33–36] In prior

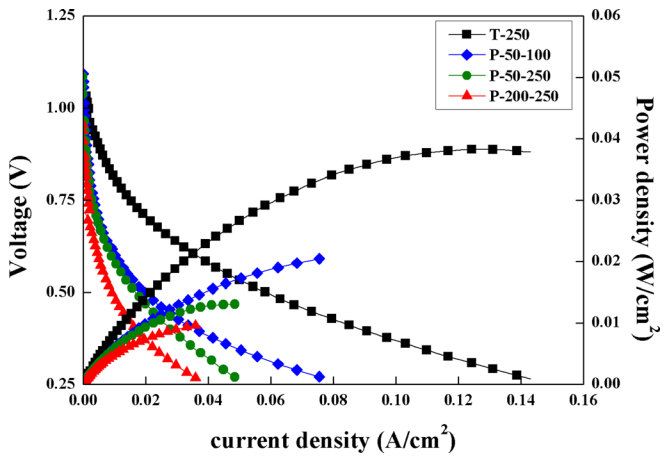

FIG. 4. (Color online) Polarization results of TF-SOFCs based on nanostructured ZrO_2 thin film electrolytes.

reports, the activation loss due to ORRs increased as the average grain size at the cathode/electrolyte interface increased. This trend arises because grain boundaries at the cathode/electrolyte interface act as preferential sites for oxygen ion incorporation reactions due to their higher concentrations of oxygen vacancies.[33–36] In the present work, the average grain size of ZrO_2 thin films increased when the PEALD was used, or when the deposition temperature, plasma power, or plasma duration increased. Despite the reduced contamination and improved crystallinity of films formed by PEALD, the increased average surface grain sizes of these ZrO_2 thin films induced larger cathodic activation loss and therefore lower peak power density.

To investigate the electrochemical characteristics of the TF-SOFCs, fuel cells based on the T-250 and P-50-250 films were analyzed by EIS. Figure 5(a) shows the semicircles representing polarization resistance at electrodes (mostly at the cathode side considering the low operating temperature[1]) for two samples: TF-SOFC with T-250 (i.e., small grains and high density of grain boundaries) and that with P-50-250 (i.e., large grains and low density of grain boundaries) at 0.5 V DC biased conditions [Fig. 5(a)]. Figure 5(b) compares

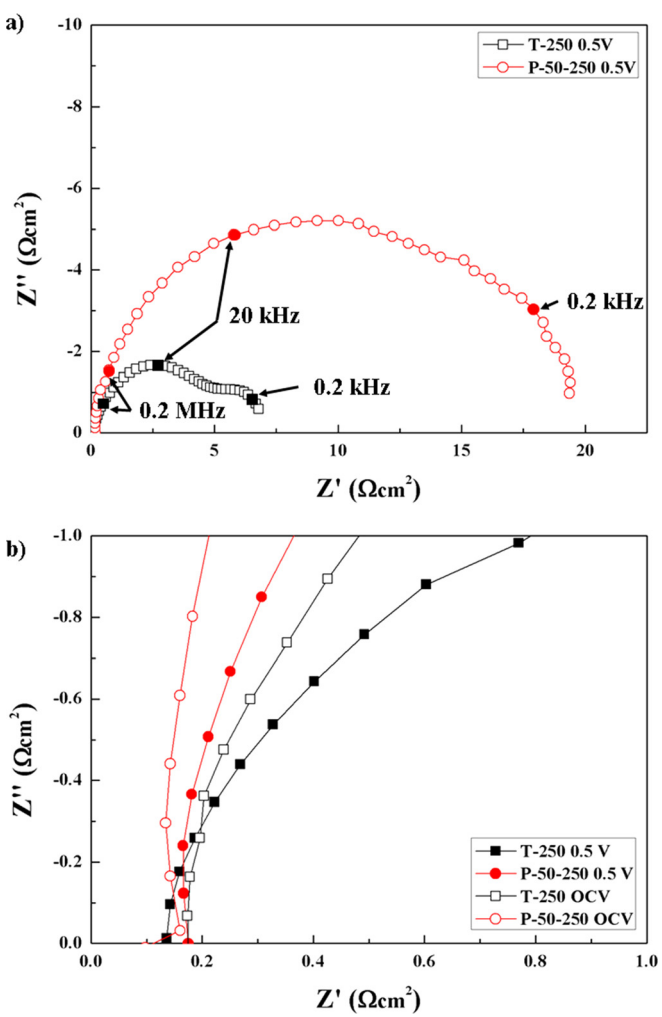

FIG. 5. (Color online) EIS results of TF-SOFCs. (a) EIS results of TF-SOFCs based on nanostructured ZrO_2 thin film electrolytes, operated at 0.5 V DC bias. (b) Ohmic resistance of TF-SOFCs.

the ohmic resistance, that is, the intercept point of the real axis (X axis) measured under OCV conditions and 0.5 V DC bias conditions. The trend in electrode polarization resistances of TF-SOFCs [Fig. 5(a)] demonstrated a clear difference from the trend in ohmic resistance [Fig. 5(b)]. Considering the aforementioned average grain size of the ZrO_2 thin films, these electrode polarization resistance suggested an obvious relation between the average grain size and the cathodic polarization resistance: as the average grain size increased, the electrode polarization resistance increased.

This relation was consistent with previous findings.[33–36] The difference in the cathodic polarization resistance due to the different average grain sizes significantly affected the electrochemical performance of the TF-SOFCs, as shown in Fig. 4.

Interestingly, ohmic resistances [i.e., real axis intercepts in Fig. 5(b)] showed negligible deviation between the fuel cell samples, which implies that the ionic conductivity of the ZrO_2 films was similar to each other in spite of the variations in the impurity concentration and grain structure. The ohmic resistances, in any case, were even smaller than the cathodic polarization resistances; therefore, the fuel cell performance was not significantly affected.

According to the AFM, FIB-SEM, I–V performance, and EIS results, the difference in peak power density and EIS behavior of the TF-SOFCs was not caused by differences in cell structure or cathode status (i.e., porosity, thickness, etc.). Rather, the poor performance and high cathodic polarization resistance of the TF-SOFC based on P-50-250 appeared to be caused solely by the large average grain size (i.e., low grain boundary density) at cathode/electrolyte interface.

IV. SUMMARY AND CONCLUSIONS

ZrO_2 thin films prepared by PEALD and by a conventional thermal ALD method were studied. PEALD yielded ZrO_2 thin films with negligible impurity content, whereas conventional thermal ALD yielded the impurity content of nearly 5.5 at. % C and 2.6 at. % N due to the poor reactivity of oxygen gas in this technique. Moreover, ZrO_2 fabricated by thermal ALD had amorphous crystal structure, whereas PEALD yielded ZrO_2 of clear polycrystalline structure because of the superior reactivity of the plasma species and the additional energy provided by the oxygen plasma. The average grain size was calculated based on AFM measurements and was shown to increase when the PEALD process was used, or when the deposition temperature, plasma power, or plasma time was increased.

After characterization of the nanostructured ZrO_2 thin films, they were applied as the electrolyte layers in AAO-based TF-SOFCs. All TF-SOFCs based on the ZrO_2 thin film electrolytes showed reasonable OCV approaching the theoretical value. The performance of the TF-SOFC based on T-250 was measured to be 38 mW/cm^2 at 500 °C. Interestingly, the TF-SOFCs based on electrolytes formed by PEALD performed poorly compared to those based on electrolytes formed by thermal ALD; EIS analyses of the

PEALD films showed that they had high cathodic polarization resistances. We speculated that these high resistances were caused by the larger average grain size of films formed by PEALD. The results of this study may have significant implications regarding the optimization of the PEALD process for preparing thin film electrolytes for use in TF-SOFCs, by clarifying the roles of grain size and deposition conditions.

ACKNOWLEDGMENTS

This work was supported by the Global Frontier R&D Program of the Center for Multiscale Energy System, funded by the National Research Foundation under the Ministry of Education, Science and Technology of Korea (2011-0031569). BK21 Plus is also acknowledged for their partial support.

[1]J. An, Y. B. Kim, J. Park, T. M. Gür, and F. B. Prinz, Nano Lett. **13**, 4551 (2013).
[2]J. H. Shim, C. C. Chao, H. Huango, and F. B. Prinz, Chem. Mater. **19**, 3850 (2007).
[3]J. H. Shim *et al.*, J. Mater. Chem. A **1**, 12695 (2013).
[4]C. Ko, K. Kerman, and S. Ramanathan, J. Power Sources **213**, 343 (2012).
[5]D. Yang, X. Zhang, S. Nikumb, C. Decès-Petit, R. Hui, R. Maric, and D. Ghosh, J. Power Sources **164**, 182 (2007).
[6]Y. Jee, G. Y. Cho, J. An, H.-R. Kim, J.-W. Son, J.-H. Lee, F. B. Prinz, M. H. Lee, and S. W. Cha, J. Power Sources **253**, 114 (2014).
[7]Y. Yoo, J. Power Sources **160**, 202 (2006).
[8]D. Virbukas, G. Laukaitis, J. Dudonis, O. Katkauske, and D. Milčius, Solid State Ionics **184**, 10 (2011).
[9]S. Ji, I. Chang, Y. H. Lee, J. Park, J. Y. Paek, M. H. Lee, and S. W. Cha, Nanoscale Res. Lett. **8**, 48 (2013).
[10]B.-K. Lai, K. Kerman, and S. Ramanathan, J. Power Sources **195**, 5185 (2010).
[11]S. Hong, J. Bae, B. Koo, and Y.-B. Kim, Electrochem. Commun. **47**, 1 (2014).
[12]S. Ji, I. Chang, G. Y. Cho, Y. H. Lee, J. H. Shim, and S. W. Cha, Int. J. Hydrogen Energy **39**, 12402 (2014).
[13]J. Park, I. Chang, J. Y. Paek, S. Ji, W. Lee, S. W. Cha, and J. M. Lee, CIRP Ann. Manuf. Technol. **63**, 513 (2014).
[14]M. J. Weber, A. J. M. MacKus, M. A. Verheijen, C. Van Der Marel, and W. M. M. Kessels, Chem. Mater. **24**, 2973 (2012).
[15]M. Tsuchiya, B. Lai, and S. Ramanathan, Nat. Nanotechnol. **6**, 282 (2011).
[16]P. Su, C. Chao, J. H. Shim, R. Fasching, and F. B. Prinz, Nano Lett. **8**, 2289 (2008).
[17]I. Garbayo, D. Pla, A. Morata, L. Fonseca, N. Sabate, and A. Tarancon, Energy Environ. Sci. **7**, 3617 (2014).
[18]C. Kwon, J. Son, J. Lee, H. Kim, H. Lee, and K. Kim, Adv. Funct. Mater. **21**, 1154 (2011).
[19]C. N. Ginestra, R. Sreenivasan, A. Karthikeyan, S. Ramanathan, and P. C. McIntyre, Electrochem. Solid-State Lett. **10**, B161 (2007).
[20]C. C. Chao, J. S. Park, X. Tian, J. H. Shim, T. M. Gür, and F. B. Prinz, ACS Nano **7**, 2186 (2013).
[21]Y. Gong, D. Palacio, X. Song, R. L. Patel, X. Liang, X. Zhao, J. B. Goodenough, and K. Huang, Nano Lett. **13**, 4340 (2013).
[22]Y. Gong, R. L. Patel, X. Liang, D. Palacio, X. Song, J. B. Goodenough, and K. Huang, Chem. Mater. **25**, 4224 (2013).
[23]S. J. Yun, J. W. Lim, and J. H. Lee, Electrochem. Solid-State Lett. **8**, F47 (2005).
[24]D. Chan Won and S.-W. Rhee, J. Vac. Sci. Technol. B **32**, 03D102 (2014).
[25]Y. Duan, F. Sun, Y. Yang, P. Chen, D. Yang, Y. Duan, and X. Wang, ACS Appl. Mater. Interfaces **6**, 3799 (2014).
[26]H. B. Profijt, S. E. Potts, M. C. M. van de Sanden, and W. M. M. Kessels, J. Vac. Sci. Technol. A **29**, 050801 (2011).
[27]H. Kim, Thin Solid Films **519**, 6639 (2011).
[28]J. An, T. Usui, M. Logar, J. Park, D. Thian, S. Kim, K. Kim, and F. B. Prinz, ACS Appl. Mater. Interfaces **6**, 10656 (2014).
[29]E. Djurado, P. Bouvier, and G. Lucazeau, J. Solid State Chem. **149**, 399 (2000).
[30]G. Baldinozzi, D. Simeone, D. Gosset, and M. Dutheil, Phys. Rev. Lett. **90**, 216103 (2003).
[31]Y. B. Kim, J. H. Shim, T. M. Guür, and F. B. Prinz, J. Electrochem. Soc. **158**, B1453 (2011).
[32]Y. B. Kim, J. S. Park, T. M. Gür, and F. B. Prinz, J. Power Sources **196**, 10550 (2011).
[33]J. H. Shim, J. S. Park, T. P. Holme, K. Crabb, W. Lee, Y. B. Kim, X. Tian, T. M. Gür, and F. B. Prinz, Acta Mater. **60**, 1 (2012).
[34]C.-C. Chao, Y. B. Kim, and F. B. Prinz, Nano Lett. **9**, 3626 (2009).
[35]W. Lee, H. J. Jung, M. H. Lee, Y. B. Kim, J. S. Park, R. Sinclair, and F. B. Prinz, Adv. Funct. Mater. **22**, 965 (2012).
[36]J. Bae, S. Hong, B. Koo, J. An, F. B. Prinz, and Y. B. Kim, J. Eur. Ceram. Soc. **34**, 3763 (2014).